# Effects of Channel Wall Thickness between Primary and Secondary Channels on Thermal Performance of Printed Circuit Steam Generators

Seok Kim [a*], Sang Ji Kim [a]
[a]*Korea Atomic Energy Research Institute, 111 Daedeok-daero 989beon-gil, Yuseong-gu, Daejeon, 34057, Republic of Korea*
[*]*Corresponding author: seokkim@kaeri.re.kr*

## 1. Introduction

Small integral-type reactors need to reduce sizes of its reactor vessel and components for movability and economic efficiency for its construction. The biggest component in the reactor vessel of SMART (System-integrated Modular Advanced ReacTor) developed by KAERI (Korea Atomic Energy Research Institute) is a shell-and-tube type steam generator [1]. Innovative miniaturization of the steam generator would result in downsizing of the reactor vessel, thereby it enables its transportation by land and reduction of manufacturing costs.

A PCSG (Printed Circuit Steam Generator) is a most innovative one of the alternatives to the shell-and-tube type steam generator. Heat transfer rate per unit volume of the PCSG is much higher than the conventional heat exchangers, and its structure is robust due to the diffusion bonding technique. Therefore the PCSG is a strong candidate for the innovative steam generator in SMART.

To size the PCSG for SMART, the methodology for performance evaluation of the PCSG was developed by adopting thermal-hydraulic analysis of a unit channel [2]. In this study, effects of a channel wall thickness between primary and secondary channels on thermal performance of the PCSG is investigated by using the methodology.

## 2. Numerical Method

The methodology for evaluating thermal performance of PCSGs was already described in another paper [2] written by the authors of this paper. However, its description was very brief due to lack of space and it was written in Korean. Thus, the main concept, assumptions and equations of the methodology are again presented in detail in this paper to encourage to spread and share the methodology.

### *2.1 Unit Channel*

A PCSG is manufactured by repeatedly stacking plates where primary-side channels and secondary-side channels are etched, and the channels of each side have the same geometry. Therefore, a repetitive pattern of the channels can be shown on the cross-section of the PCSG as depicted in Fig. 1. The pattern gives thermally symmetric interfaces, and a unit channel focused in this numerical method is defined as a region around a primary channel and surrounded by the thermally symmetric interfaces. Fortunately, it enables disregard for heat transfer through boundaries of the unit channel, so that it is unnecessary to calculate millions of the channels one by one.

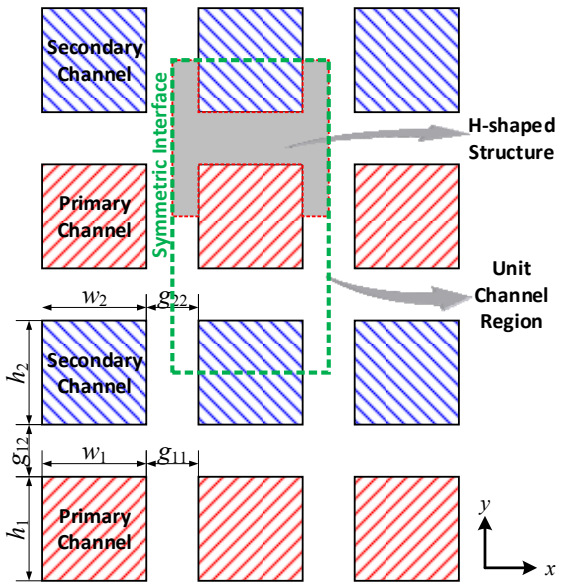


Fig. 1. Unit channel and its geometries on the cross-section of the PCSG.

For the representability of the unit channel for thermal performance of the PCSG, it should be assumed that flow distribution through the primary channels and the secondary channels are even, respectively. Only then each channel experiences an equivalent thermal load.

### *2.2 Thermal Network Model*

To obtain the temperature and pressure distribution along the flow direction, the unit channel is discretized one-dimensionally as shown in Fig. 2, and the finite volume method is adopted to discretized nodes of primary and secondary channels. Here, heat transfer rate ($q$) from the primary channel to the secondary channel for a discretized node is caused by the temperature difference ($T_1 - T_2$) between the channels against the primary-side convective thermal resistance ($R_{conv1}$), the structural conductive thermal resistance ($R_{cond}$) and the secondary-side convective thermal resistance ($R_{conv2}$) as follows:

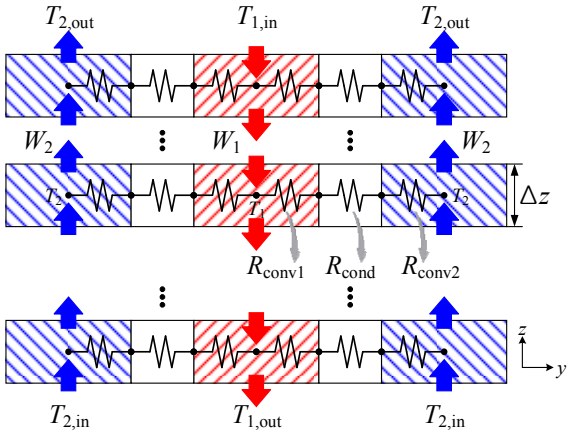


Fig. 2. One-dimensional discretization of unit channel and thermal network model.

$$q = \frac{T_1 - T_2}{\left(R_{conv1} + R_{cond} + R_{conv2}\right)/2} \tag{1}$$

$$R_{conv1} = \frac{1}{H_1\left[w_1\Delta z + 2\left(h_1/2\right)\Delta z\right]} \tag{2}$$

$$R_{cond} = \frac{R_{cond}A_{stack}}{\left(g_{11}/2 + w_1 + g_{11}/2\right)\Delta z} \tag{3}$$

$$R_{conv2} = \frac{1}{H_2\left(w_2\Delta z + 2\left(h_2/2\right)\Delta z\right)} \tag{4}$$

where $H_1$ and $H_2$ are primary- and secondary-side heat transfer coefficients, respectively, and $R_{cond}A_{stack}$ is the area-based conductive thermal resistance, which is devised to calculate the structural conductive thermal resistance by dividing $R_{cond}A_{stack}$ by a specific cross-sectional area in $y$-plane of a discretized node of the unit channel [3]. The area-based conductive thermal resistances were obtained as a function of $H_1$ and $H_2$ for the specific H-shaped structure with different channel wall thickness between primary and secondary channels ($g_{12}$) as shown in Fig. 1.

### *2.3 Heat Transfer Coefficient*

For single-phase flow, the analytic solution for laminar flow, and Dittus and Boelter's heat transfer coefficient [4] for turbulent flow are used as follows:

$$H = \begin{cases} 3.61\dfrac{k}{D} & \text{for laminar} \\ 0.023\,\mathrm{Re}^{0.8}\,\mathrm{Pr}^{0.4}\dfrac{k}{D} & \text{for turbulent} \end{cases} \tag{5}$$

Whereas Kandlikar's heat transfer coefficient [5] is adopted for two-phase flow, and its correlation is given as:

$$H = MAX\left(H_{NBD}, H_{CBD}\right) \tag{6}$$

$$H_{NBD} = H_{fo}\begin{bmatrix} 0.6683\mathrm{Co}^{-0.2}\left(1-x\right)^{0.8} f_2\left(\mathrm{Fr}_{fo}\right) \\ +1058.0\mathrm{Bo}^{0.7}\left(1-x\right)^{0.8} F_{fl} \end{bmatrix} \tag{7}$$

$$H_{CBD} = H_{fo}\begin{bmatrix} 1.136\mathrm{Co}^{-0.9}\left(1-x\right)^{0.8} f_2\left(\mathrm{Fr}_{fo}\right) \\ +667.2\mathrm{Bo}^{0.7}\left(1-x\right)^{0.8} F_{fl} \end{bmatrix} \tag{8}$$

where $x$, Co, Bo and $\mathrm{Fr}_{fo}$ are the convection number, the boiling number and the Froude number when all mixture is saturated liquid, defined, respectively, as:

$$\mathrm{Co} = \left(\rho_g/\rho_f\right)^{0.5}\left[\left(1-x\right)/x\right]^{0.8} \tag{9}$$

$$\mathrm{Bo} = q''/\left(G\cdot i_{fg}\right) \tag{10}$$

$$\mathrm{Fr}_{fo} = G^2/\left(\rho_f^2 gD\right) \tag{11}$$

Here, $i$, $\rho$, $q''$, $G$, $g$ and $D$ means enthalpy, density, wall heat flux, mass flux, gravitational acceleration and hydraulic diameter, respectively, and the subscripts f and g indicate liquid-phase and gas-phase, respectively. Moreover, the parameter, $F_{fl}$, in Eqs. (7) and (8) is the fluid-surface parameter, and 1.00 for water. For vertical tubes and for horizontal tubes with $\mathrm{Fr}_{fo} \geq 0.4$, $f_2(\mathrm{Fr}_{fo}) = 1$, otherwise, $f_2(\mathrm{Fr}_{fo}) = (25\mathrm{Fr}_{fo})^{0.3}$ for $\mathrm{Fr}_{fo} < 0.4$ in horizontal tubes. For the calculation of $H_{fo}$, the analytic solution for laminar flow and the Gnielinski's correlation [6] for turbulent flow are recommended as:

$$H_{fo} = \begin{cases} 3.61\dfrac{k}{D} & \text{for laminar} \\ \dfrac{\left(\mathrm{Re}_{fo}-1000\right)\left(\dfrac{f'}{2}\right)\mathrm{Pr}_f}{\left[1+12.7\left(\mathrm{Pr}_f^{\frac{2}{3}}-1\right)\left(\dfrac{f'}{2}\right)^{\frac{1}{2}}\right]}\dfrac{k}{D} & \text{for turbulent} \end{cases} \tag{12}$$

where $\mathrm{Re}_{fo}$ is the Reynolds number when all mixture is assumed to be saturated liquid, and $\mathrm{Pr}_f$ and $k$ are the Prandtl number and thermal conductivity of liquid, respectively. Also, the Petukhov's friction factor correlation [7] is used as $f'$, as following:

$$f' = \left[1.58\ln\left(\mathrm{Re}_{fo}\right) - 3.28\right]^{-2} \tag{13}$$

### *2.4 Pressure Drop*

The pressure drop gradient for single-phase flow can be written as:

$$-\frac{\mathrm{d}p}{\mathrm{d}z} = -\left(\frac{\mathrm{d}p}{\mathrm{d}z}\right)_F - \left(\frac{\mathrm{d}p}{\mathrm{d}z}\right)_G \tag{14}$$

where $(-\mathrm{d}p/\mathrm{d}z)_F$ and $(-\mathrm{d}p/\mathrm{d}z)_G$ are the frictional and the gravitational pressure drop gradients, respectively, which are derived as follows:

$$-\left(\frac{\mathrm{d}p}{\mathrm{d}z}\right)_{\mathrm{F}} = 2f\frac{G^2}{\rho D} \tag{15}$$

$$-\left(\frac{\mathrm{d}p}{\mathrm{d}z}\right)_{\mathrm{G}} = \rho g\sin\theta \tag{16}$$

Here, $\theta$ is an inclination angle of the channel, and the friction factor, $f$, can be obtained as:

$$f = \begin{cases} 16/\mathrm{Re} & \text{for laminar} \\ 0.079\,\mathrm{Re}^{-0.25} & \text{for turbulent} \end{cases} \tag{17}$$

Next, for two-phase flow, the accelerational pressure drop gradient is added to the single-phase flow pressure drop gradient as follows:

$$-\frac{\mathrm{d}p}{\mathrm{d}z} = -\left(\frac{\mathrm{d}p}{\mathrm{d}z}\right)_{\mathrm{F}} - \left(\frac{\mathrm{d}p}{\mathrm{d}z}\right)_{\mathrm{G}} - \left(\frac{\mathrm{d}p}{\mathrm{d}z}\right)_{\mathrm{A}} \tag{18}$$

where each pressure drop gradient for two-phase flow can be calculated as:

$$-\left(\frac{\mathrm{d}p}{\mathrm{d}z}\right)_{\mathrm{F}} = 2f_{\mathrm{f}}\frac{G^2(1-x)^2}{\rho D}\phi_{\mathrm{f}}^2 \tag{19}$$

$$-\left(\frac{\mathrm{d}p}{\mathrm{d}z}\right)_{\mathrm{G}} = \rho g\sin\theta \tag{20}$$

$$-\left(\frac{\mathrm{d}p}{\mathrm{d}z}\right)_{\mathrm{A}} = G^2\left(\frac{1}{\rho_{\mathrm{g}}} - \frac{1}{\rho_{\mathrm{f}}}\right)\frac{\mathrm{d}x}{\mathrm{d}z} \tag{21}$$

Here, $\phi_{\mathrm{f}}^2$ is the two-phase flow frictional pressure drop multiplier, and can be obtained as:

$$\phi_{\mathrm{f}}^2 = 1 + \frac{C}{X} + \frac{1}{X^2} \tag{22}$$

$$X^2 = \frac{f_{\mathrm{f}}(1-x)^2/\rho_{\mathrm{f}}}{f_{\mathrm{g}}x^2/\rho_{\mathrm{g}}} \tag{23}$$

$$C = 21\left(1 - e^{-0.319D/1000}\right) \tag{24}$$

Finally, the pressure drop for a discretized node is as follows:

$$\Delta p = -\frac{\mathrm{d}p}{\mathrm{d}z}\cdot\Delta z \tag{25}$$

*2.5 Energy Balance*

Discretized energy conservation equations for each node of primary and secondary sides are derived as:

$$i_{1,\mathrm{in}}W_{1,\mathrm{in}} - i_{1,\mathrm{out}}W_{1,\mathrm{out}} = q \quad \text{for primary channel} \tag{26}$$

$$i_{2,\mathrm{in}}W_{2,\mathrm{in}} - i_{2,\mathrm{out}}W_{2,\mathrm{out}} = -q \quad \text{for secondary channel} \tag{27}$$

*2.6 Algorithm*

The algorithm of the unit channel thermal-hydraulic analysis code for performance evaluation of PCSG is presented in Fig. 3. For initiation of a calculation, the geometries of the primary and secondary channels shown in Fig. 1, channel length, channel quantity, node quantity and boundary conditions should be given. Once the channels length is discretized by the node quantity, the thermal resistances, heat flow rate and heat transfer coefficient are calculated. Then pressure and enthalpy distribution along the flow direction can be obtained through pressure drop and energy balance equations, respectively, and temperature distribution is also calculated based on the pressure and the enthalpy [9]. If the pressure and the enthalpy distribution is not converged, repeated calculation of above procedure will give the final converged solution.

## 3. Results

In this study, two channel arrangement types with different channel wall thickness between primary and secondary channels as shown in Fig. 4 are evaluated. The channel wall thickness ($g_{12}$) of Type A is 1.0 mm, meanwhile, 2.0 mm for Type B, but, except for the channel wall thickness, other geometries, such as the channel size and the gap of each side, are equivalent, and channel quantity of each side and channel length are same to be 107,000 and 2.0 m, respectively. Moreover, all of the calculation conditions are same, for example, the primary- and secondary-side flow rates, inlet temperatures and inlet pressures. Finally, primary and secondary fluids flow in opposite direction.

Fig. 5 shows thermal resistance distributions along the flow direction for Type A and Type B. This values of the thermal resistance are based on a discretized node ($\Delta z$ = 5 mm) of the unit channel. The increase in

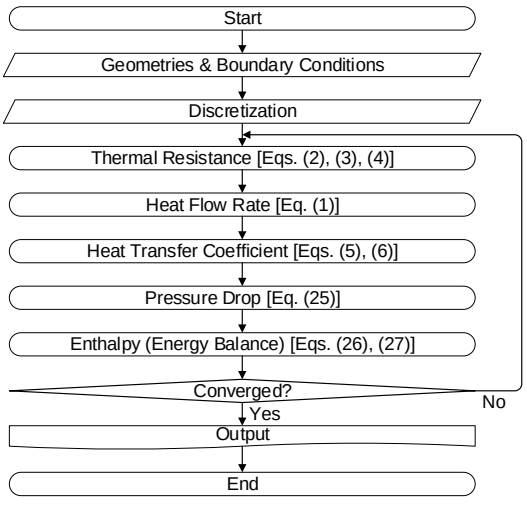


Fig. 3. Algorithm of unit channel thermal-hydraulic analysis code for performance evaluation of PCSG.

the channel wall thickness results in an increase in structural conductive thermal resistance. In this calculation, the change of the channel wall thickness from 1.0 mm to 2.0 mm gives approximately double conductive thermal resistance. Therefore, total thermal resistance of Type B is greater than that of Type A, so that heat transfer rate from primary side to secondary side is decreased. As a result, for type B in Fig. 6, the feedwater injected into secondary channels cannot be totally changed into superheated steam, and outlet temperature of the primary side is increased.

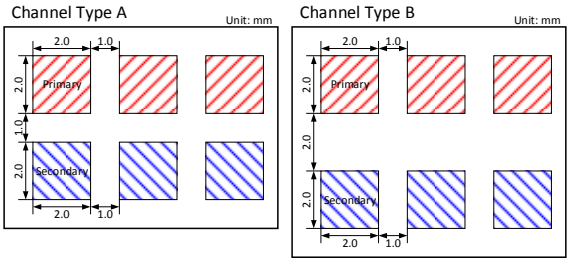


Fig. 4. Channel arrangement types – Type A: $g_{12}$ = 1.0 mm, Type B: $g_{12}$ = 2.0 mm.

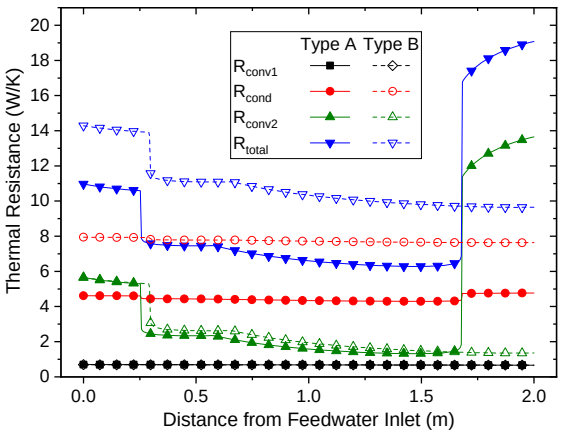


Fig. 5. Thermal resistance distributions.

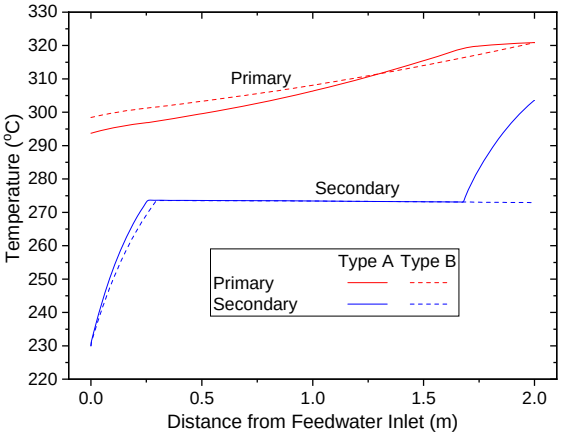


Fig. 6. Temperature distributions.

## 4. Conclusions

In this study, effects of channel wall thickness between primary and secondary channels of a PCSG is evaluated. An increase in the channel wall thickness results in a decrease in heat transfer rate per a unit channel, and more channels for equivalent thermal performance of the PCSG. However, because too thin channel wall may occur failure of pressure boundary between primary and secondary sides, it is essential to evaluate its structural integrity.

## Acknowledgement

This work was supported by the National Research Foundation (NRF) of Korea funded by the Ministry of Science and ICT, South Korea (2018M2A8A4081307).

## REFERENCES

[1] SMART Standard Design Safety Analysis Report, KAERI, 2012.
[2] S. Kim, Y. I. Kim, S. J. Kim, Methodology of Unit Channel Thermal-Hydraulic Analysis for Performance Evaluation of Printed Circuit Steam Generators, Proceedings of the KSME Fluid Engineering Division 2019 Spring Conference, Gangneung, pp. 221-222, 2019.
[3] H. Cho, Y. Bae, C. B. Chang, S. Kim, J. Kee, M. Lee, Y. I. Kim, S. J. Kim, A Preliminary CFD Analysis for Application of a Printed Circuit Steam Generator for SMART, KAERI, KAERI/TR-7600/2019, pp. 75, 2019.
[4] F. W. Dittus, L. M. K. Boelter, Heat Transfer in Automobile Radiators of the Tubular Type, University of California Publications on Engineering, Vol. 2, pp. 443-461, 1930.
[5] S. G. Kandlikar, A General Correlation for Saturated Two-Phase Flow Boiling Heat Transfer inside Horizontal and Vertical Tubes, Journal of Heat Transfer, Vol. 112, pp. 219-228, 1990.
[6] V. Gnielinski, New equations for heat and mass transfer in turbulent pipe and channel flow, International Journal of Chemical Engineering, Vol. 16, pp. 359-368, 1976.
[7] B. S. Petukhov, Heat transfer and friction in turbulent pipe flow with variable physical properties, Advanced Heat Transfer, Vel. 6, pp. 503-565, 1970.
[8] R. W. Lockhart, R. C. Martinelli, Proposed correlations of data for isothermal two-phase, two-component flow in a pipe, Chemical Engineering Progress, Vol. 45, pp. 39-48, 1949.
[9] E. W. Lemmon, M. L. Huber, M. O. McLinden, Reference Fluid Thermodynamic and Transport Properties (REFPROP), Ver 9.0, NIST, 2010.